

# Photon propagation in a cold axion background and strong magnetic fields: interferometric and polarimetric experiments

Domènec Espriu<sup>1</sup> and Albert Renau<sup>1</sup>

<sup>1</sup>*Departament d'Estructura i Constituents de la Matèria,*

*Institut de Ciències del Cosmos (ICCUB),*

*Universitat de Barcelona, Martí Franquès 1, 08028 Barcelona, Spain*

## Abstract

In this work we analyze the propagation of photons in an environment where a strong magnetic field (perpendicular to the photon momenta) coexists with an oscillating cold axion background with the characteristics expected from dark matter in the galactic halo. Qualitatively, the main effect of the combined background is to produce a three-way mixing among the two photon polarizations and the axion. It is interesting to note that in spite of the extremely weak interaction of photons with the axion background, its effects may compete with those coming from the magnetic field in some regions of the parameter space. We determine (with one plausible simplification) the proper frequencies and eigenvectors, and the corresponding photon ellipticities that depend both on the magnetic field and the local density of axions. We also comment on the feasibility of interferometric and polarimetric table-top experiments to detect the latter.

## I. INTRODUCTION

Originally introduced to solve the strong  $CP$  problem [1], axions are an attractive and viable candidate for dark matter (DM) [2, 3]. The axion is the Goldstone boson associated with the spontaneous breaking of the  $U(1)_{PQ}$  symmetry[1]. After the QCD phase transition, instanton effects induce a potential on the axion field, giving it a mass  $m_a$ . Cosmological constraints (see below) force this mass to be quite small. Yet, the axion provides cold dark matter, as it is not produced thermically. If the axion background field is initially misaligned (not lying at the bottom of the instanton-induced potential), at late times it oscillates coherently as

$$a_b(t) = a_0 \sin m_a t, \quad (1)$$

where the amplitude,  $a_0$ , is related to the initial misalignment angle. The oscillation of the axion field has an approximately constant (i.e. momentum-independent) energy density  $\rho = \frac{1}{2}a_0^2 m_a^2$ , which contributes to the total energy of the universe<sup>1</sup>. This constitutes the cold axion background (CAB for short). There are suggestions that axions could actually form a Bose-Einstein condensate [4].

Axions couple to photons through the universal term

$$\mathcal{L}_{a\gamma\gamma} = g_{a\gamma\gamma} \frac{\alpha}{2\pi} \frac{a}{f_a} F_{\mu\nu} \tilde{F}^{\mu\nu}, \quad (2)$$

where the coefficient  $g_{a\gamma\gamma}$  does depend on the model<sup>2</sup>. However, most of them [5] give  $g_{a\gamma\gamma} \simeq 1$ . For the present discussion this is all that matters. The universality of the axion-photon coupling makes it the best candidate to explore axion physics.

Cosmology considerations place the axion mass in the range  $10^{-2} - 10^{-6}$  eV. In the case of Peccei-Quinn axions, the approximate relation  $f_a m_a \simeq f_\pi m_\pi$  should hold, which implies the bound  $f_a > 10^9$  GeV. For other axion-like particles, not related to the strong  $CP$  problem, there is no such relation and the range of possible values is more open, although a lot less motivated from a physical point of view. The limit  $f_a > 10^7$  GeV coming from astrophysics seems now well established, in any case. If one assumes that axions are the main ingredient of DM, there is also an upper bound:  $f_a < 3 \cdot 10^{11}$  GeV. See [3] and references therein for

---

<sup>1</sup> This density is not really constant, as DM tends to concentrate in galactic halos. Nevertheless it changes over very large scales, so for our purposes it suffices to treat it as a constant.

<sup>2</sup> Sometimes a dimensionful coupling constant  $G_{a\gamma\gamma} \propto \frac{1}{f_a}$  is used instead. Our  $g_{a\gamma\gamma}$  is dimensionless.

an explanation of the above bounds. These values of  $f_a$  make the axion very weakly coupled and imply a very long lifetime, of the order of  $10^{24}$  years or more; see e.g. [6].

Axions could also couple to matter, although in this case the coupling is much more model dependent. However, the coupling is so small that their detection is very difficult. Nevertheless, some of the best bounds on axion masses and couplings come from the study of abnormal cooling in white dwarfs due to axion emission [7].

When dealing with axions and their possible cosmological relevance, there are several separate issues that have to be addressed. The first one is whether axions exist or not at all. This is what experiments such as CAST [8], ADMX, ADMX Phase II [9], IAXO [10] or ALPS [11] are addressing directly. If the axion does exist and its mass happens to be in the relevant range for cosmology we would have a strong hint that axions may serve as valid DM candidates. The ADMX experiment [9] tries to detect axions in the Galaxy dark matter halo that, under the influence of a strong magnetic field, would convert to photons with a frequency equal to the axion mass. This experiment is sensitive to the local axion density, the probability of a positive detection being proportional to the latter.

However, finding an axion particle with the appropriate characteristics or even finding a non-zero local density is strictly speaking not enough to demonstrate that a CAB exists. For a CAB to be present one needs to make sure that dark matter axions oscillate in phase, rather than incoherently. Clearly, a direct experimental confirmation of the CAB is very important but extremely difficult and is not within reach of any of the above experiments.

Looking for the collective effects on photon propagation resulting from the presence of a CAB is a possibility that needs careful examination in order to determine whether there is a CAB around us. Of course we do not anticipate large or dramatic effects given the presumed smallness of the photon-to-axion coupling and the very diffuse background that a CAB would provide. However, interferometric and polarimetric techniques are very powerful and it is interesting to explore the order of magnitude of the different effects.

It is worth noting that a CAB introduces via its time dependence some amount of Lorentz-invariance violation in photon physics; the term (2) does actually modify the photon dispersion relation and it has somewhat exotic consequences. For instance, in [12] we showed how this modification of the dispersion relation allows the emission of a photon by a cosmic ray, a process forbidden due to conservation of energy and momentum in a Lorentz-invariant theory. In [13] we computed the amount of energy radiated by this process and found it to be

non-negligible, although the normal synchrotron radiation background makes its detection very challenging.

In [14] we found that some photon wave numbers are actually forbidden in a CAB, as a consequence of its time dependence. This striking result is an unavoidable and direct consequence of the periodicity of the CAB oscillations. Unfortunately, as we will see, the width of the forbidden momentum bands is very small and its detection very challenging for axions of cosmological relevance. In [14] we also provided some results on the propagation of photons under the simultaneous influence of a CAB and a magnetic field.

It is well known that photons polarized in a direction perpendicular to the magnetic field are not affected by the existence of axions [15]; only photons polarized in the parallel direction mix with them. As a consequence there is a small rotation in the polarization plane due to photon-axion mixing as well as a change in the ellipticity [16]. In [14] we showed that a similar effect exists even without a magnetic field when a CAB is present except that now it involves the two photon helicities. Again the effect is very small as we will discuss below.

In this paper we continue our investigation on the propagation of photons in the presence of both a CAB and an external magnetic field. In section II we review the problem and derive the equations of motion for the axion and photon in the presence of both backgrounds, both for linear and circular polarization bases for the photon. In section III we discuss the results for the case of no magnetic field and show the appearance of gaps in the photon momenta; adding more details to those already provided in [14] such as the width of the gaps. In sections IV and V we study the consequences that the combined background has on photon frequencies and polarizations. We also investigate to what extent the predicted effects could be measurable in interferometric experiments. In section VI we explore the consequences of the change in the plane of polarization of the photons in the presence of the CAB. The technical details are given in a detailed appendix. A short summary of some of our results was already presented in [17].

## II. EQUATIONS OF MOTION OF THE AXION-PHOTON SYSTEM

The Lagrangian density describing axions and photons consists of the usual kinetic terms plus the interaction term (2)

$$\mathcal{L} = \frac{1}{2}\partial_\mu a \partial^\mu a - \frac{1}{2}m_a^2 a^2 - \frac{1}{4}F_{\mu\nu}F^{\mu\nu} + \frac{g}{4}aF_{\mu\nu}\tilde{F}^{\mu\nu}, \quad (3)$$

where we have rewritten the axion-photon coupling as  $g = g_{a\gamma\gamma} \frac{2\alpha}{\pi f_a}$ . We are not considering the non-linear effects due to the Euler-Heisenberg Lagrangian [18] that actually can provide some modifications in the polarization plane. Later in this section we shall discuss their relevance.

We decompose the fields as a classical piece describing the backgrounds (external magnetic field  $\vec{B}$  and a CAB as given in (1)) plus quantum fluctuations describing the photon and the axion particles, e.g.  $a \rightarrow a_b + a$ . For the (quantum) photon field, we work in the Lorenz gauge,  $\partial_\mu A^\mu = 0$ , and use the remaining gauge freedom to set  $A^0 = 0$ . The equations of motion are

$$\begin{aligned} (\partial_\mu \partial^\mu + m_a^2)a + gB^i \partial_t A_i &= 0, \\ \partial_\mu \partial^\mu A^i + gB^i \partial_t a + \eta \epsilon^{ijk} \partial_j A_k &= 0. \end{aligned} \quad (4)$$

where  $\eta = g \partial_t a_b$ . Since  $\eta$  is time-dependent, we make a Fourier transform with respect to the spatial coordinates only,

$$\phi(t, \vec{x}) = \int \frac{d^3 k}{(2\pi)^3} e^{i\vec{k} \cdot \vec{x}} \hat{\phi}(t, \vec{k}), \quad (5)$$

and get the equations

$$\begin{aligned} (\partial_t^2 + \vec{k}^2 + m_a^2)\hat{a} + gB^i \partial_t \hat{A}_i &= 0, \\ (\partial_t^2 + \vec{k}^2)\hat{A}^i + gB^i \partial_t \hat{a} + i\eta \epsilon^{ijk} k_j \hat{A}_k &= 0. \end{aligned} \quad (6)$$

As can be seen, the presence of a magnetic field mixes the axion with the photon. To proceed further, we write the photon field as

$$\hat{A}_\mu(t, \vec{k}) = \sum_\lambda f_\lambda(t) \varepsilon_\mu(\vec{k}, \lambda), \quad (7)$$

where  $\varepsilon_\mu$  are the polarization vectors and  $f_\lambda(t)$  are the functions we will have to solve for.

If we choose a linear polarization basis for the photon, the equations are in matrix form

$$\begin{pmatrix} \partial_t^2 + k^2 + m_a^2 & -ib\partial_t & 0 \\ -ib\partial_t & \partial_t^2 + k^2 & -\eta(t)k \\ 0 & -\eta(t)k & \partial_t^2 + k^2 \end{pmatrix} \begin{pmatrix} \hat{a} \\ if_\parallel \\ f_\perp \end{pmatrix} = \begin{pmatrix} 0 \\ 0 \\ 0 \end{pmatrix}, \quad (8)$$

where  $k = |\vec{k}|$  and  $b = g|\vec{B}^\perp|$ , where  $\vec{B}^\perp$  is the component of the magnetic field perpendicular to the momentum (the parallel component does not affect propagation at all if the Euler-Heisenberg piece is neglected). The subscripts  $\parallel$  and  $\perp$  refer to parallel or perpendicular to this  $\vec{B}^\perp$ .

In a circular polarization basis, defining

$$f_{\pm} = \frac{f_{\parallel} \pm if_{\perp}}{\sqrt{2}}, \quad (9)$$

the equations take the form

$$\begin{pmatrix} \partial_t^2 + k^2 + m_a^2 & i\frac{b}{\sqrt{2}}\partial_t & i\frac{b}{\sqrt{2}}\partial_t \\ i\frac{b}{\sqrt{2}}\partial_t & \partial_t^2 + k^2 + \eta(t)k & 0 \\ i\frac{b}{\sqrt{2}}\partial_t & 0 & \partial_t^2 + k^2 - \eta(t)k \end{pmatrix} \begin{pmatrix} i\hat{a} \\ f_+ \\ f_- \end{pmatrix} = \begin{pmatrix} 0 \\ 0 \\ 0 \end{pmatrix}. \quad (10)$$

As we see from the previous expressions, the presence of a CAB changes in a substantial way the mixing of photons and axions. Now all three degrees of freedom are involved.

A difference in the approach between this work and [19] is worth noting. In going from (4) to (6) we have performed a Fourier transform in space, but not in time, because the magnetic field is homogeneous but  $\eta(t)$  is time-dependent. Equation (4) in [19], however, uses a transform in time rather than in space because the CAB is not considered. Their formalism is adaptable for the treatment of non-homogeneous fields as a result.

There are several ways to deal with the periodic CAB. One possibility is to try to treat it exactly. Unfortunately this unavoidably leads to the appearance of Mathieu functions due to the sinusoidal variation of the background and the analysis becomes extremely involved. On the other hand, the substantial ingredient in the problem is the existence of periodicity itself and the fine details are not so relevant<sup>3</sup>. Therefore to keep the discussion manageable, we approximate the sinusoidal variation of the axion background  $a_b(t)$  in (1) by a piecewise linear function, see figure 1. Since  $\eta(t)$  proportional to the time derivative of  $a_b(t)$ , in this

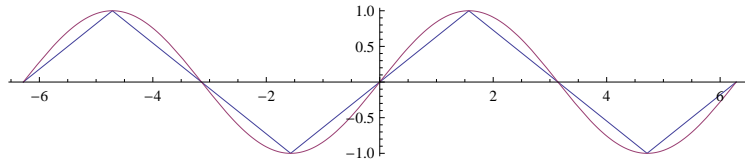


FIG. 1:  $a_b(m_a t)/a_0$  and its approximating function.

approximation it is a square-wave function, alternating between intervals where  $\eta = \eta_0$  and  $\eta = -\eta_0$  with a period  $2T = 2\pi/m_a$ . Here,  $\eta_0 = \frac{2}{\pi}ga_0m_a = g_{a\gamma\gamma}\frac{4\alpha}{\pi^2}\frac{a_0m_a}{f_a}$ .

<sup>3</sup> Recall that the generic appearance of bands in the energy levels of a solid relies on the periodicity of the potential and not on its precise details.

A brief numerical discussion of the parameters involved in the problem and their relative importance is now in order. The bound on  $f_a$  implies one on  $g$ . Taking  $g_{a\gamma\gamma}$  of  $\mathcal{O}(1)$  the range  $f_a = 10^7 - 10^{11}$  GeV translates to  $g = 10^{-18} - 10^{-22}$  eV $^{-1}$ . Assuming a halo DM density of  $\rho = 10^{-4}$  eV $^4$  [20] this means that  $\eta_0 = 10^{-20} - 10^{-24}$  eV. When working with natural units and magnetic fields it is useful to know that  $1 \text{ T} \approx 195 \text{ eV}^2$ . To have a reference value, a magnetic field of  $10 \text{ T}$  implies the range  $b = 10^{-15} - 10^{-19}$  eV, for  $f_a = 10^7 - 10^{11}$  GeV.

Finally, let us now comment on the relevance of the contribution of the Euler-Heisenberg pieces compared to the ones retained in the description provided by (3). As it is known (see e.g. [15]) an external magnetic field perpendicular to the photon motion contributes, via the Euler-Heisenberg terms, to the mixing matrices, affecting the (2,2) and (3,3) entries of (8) and (10). They modify the  $k^2$  terms with corrections of order  $10^{-2} \times \alpha^2 \times (B^2/m_e^4)$ , where  $m_e$  is the electron mass, leading to birefringence and therefore to ellipticity. For magnetic fields of  $\sim 10 \text{ T}$  this gives a contribution of order  $10^{-21}$  that may be comparable to axion-induced effects for large magnetic fields, particularly if  $f_a$  is very large, or the effects from the CAB (which for  $k \sim 1 \text{ eV}$  are in the range  $10^{-20} - 10^{-24}$ ). Since there is no new physics involved in the contribution from the Euler-Heisenberg Lagrangian, in order to facilitate the analysis we will not consider it here. In any case given the smallness of the Euler-Heisenberg and the axion effects, they can safely be assumed to be additive [15]. The relevant modifications due to the Euler-Heisenberg term can be found in [15] and [21].

Of course, the effects of the Euler-Heisenberg Lagrangian are absent or negligible if there is no magnetic field or if it is relatively weak, and we will see that for a wide range of parameters the effect of a CAB, which is independent of the magnetic field, does dominate.

### III. NO MAGNETIC FIELD: FORBIDDEN WAVELENGTHS

If there is no magnetic field ( $b = 0$ ,  $\eta_0 \neq 0$ ) the axion and the photon are no longer mixed. We explored this situation in [14] and we will summarize the main results here and complete the discussion.

Because  $\eta(t)$  does mix the two linear polarizations, in this case it is useful to choose the circular polarization basis, which diagonalizes the system. The solution is, for a given interval,  $f_{\pm}(t) = e^{i\omega_{\pm}t}$ ,  $\omega_{\pm} = \sqrt{k^2 \pm \eta_0 k}$ . Of course, when  $\eta(t)$  changes sign the solutions are interchanged as well. The way to solve this is to write  $f_{\pm}(t) = e^{i\Omega t} g_{\pm}(t)$  and demand

that  $g_{\pm}(t)$  have the same periodicity as  $\eta(t)$ . After elementary quantum mechanical considerations, periodicity of the modulus of the wave-function imposes the condition

$$\cos(2\Omega T) = \cos(\omega_+ T) \cos(\omega_- T) - \frac{\omega_+^2 + \omega_-^2}{2\omega_+ \omega_-} \sin(\omega_+ T) \sin(\omega_- T). \quad (11)$$

This condition implies the existence of momentum gaps: some values of  $k$  admit no solution for  $\Omega$ , much like some energy bands are forbidden in a semiconductor. Here, however, the roles of momentum and energy are exchanged, since the periodicity is in time, rather than in space. The solutions are shown in an  $\Omega(k)$  plot in figure 2 for two values of the ratio  $\eta_0/m_a$ . One of the ratios shown is unreasonably large, in order to show clearly the existence of the gaps.

Let us now discuss the width of these gaps, an issue that was not studied in [14] in detail. The first order in  $\eta_0$  drops from (11) but to second order it reads

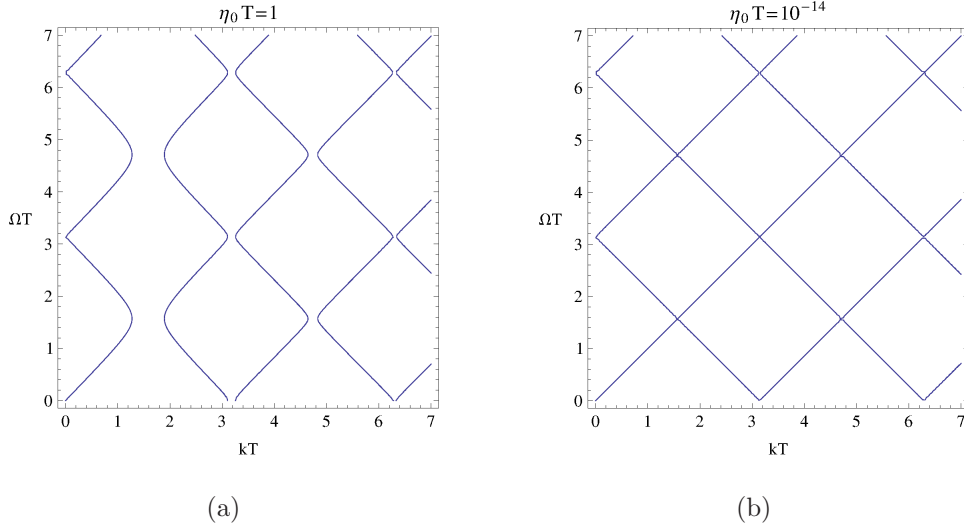


FIG. 2: Plot of the solutions to the gap equation. In the left figure the value for the ratio  $\eta_0/m_a$  is unreasonably large and it is presented here only to make the gaps in the photon momentum clearly visible.

$$\cos(2\Omega T) = \cos(2kT) + \frac{\eta_0^2}{4k^2} [-1 + \cos(2kT) + kT \sin(2kT)] \quad (12)$$

(recall that  $T = \pi/m_a$ ). There is no solution when the r.h.s. of this expression becomes larger than one. The gaps are approximately located at

$$k_n = \frac{nm_a}{2}, \quad n \in \mathbb{N} \quad (13)$$

and their width is

$$\Delta k \sim \begin{cases} \frac{\eta_0}{n\pi} & \text{for } n \text{ odd} \\ \frac{\eta_0^2}{2nm_a} & \text{for } n \text{ even} \end{cases}. \quad (14)$$

These results agree well with the exact results as can be easily seen in the left side of figure 2. Unfortunately we are not aware of any way of detecting such a tiny forbidden band for the range of values of  $\eta_0$  previously quoted ( $10^{-20}$  eV or less) that correspond to the allowed values of  $f_a$ .

It may be interesting to think what would happen if one attempts to produce a ‘forbidden’ photon, i.e. one whose momentum falls in one of the forbidden bands. A photon with such a wave number is ‘off-shell’ and as such it will always decay. For instance, it could decay into three other photons with appropriately lower energies. However, because the off-shellness is so small (typically  $10^{-20}$  eV or less) it could live for a long time as a metastable state, travelling distances commensurable with the solar system. For more technical details see e.g. [22].

#### IV. PROPER MODES IN A MAGNETIC FIELD AND AXION BACKGROUND

In the presence of a magnetic field, but no CAB ( $b \neq 0$ ,  $\eta_0 = 0$ ) there is no longer a time dependence in the coefficients of the equations, so we can Fourier transform with respect to time as well. We find the following dispersion relations:

$$\begin{aligned} \omega_a^2 &= k^2 + \frac{m_a^2 + b^2}{2} + \frac{1}{2}\sqrt{(m_a^2 + b^2)^2 + 4b^2k^2} \approx (k^2 + m_a^2) \left(1 + \frac{b^2}{m_a^2}\right) \\ \omega_1^2 &= k^2 + \frac{m_a^2 + b^2}{2} - \frac{1}{2}\sqrt{(m_a^2 + b^2)^2 + 4b^2k^2} \approx k^2 \left(1 - \frac{b^2}{m_a^2}\right) \\ \omega_2^2 &= k^2, \end{aligned} \quad (15)$$

where the  $\approx$  symbol indicates the limit  $\frac{bk}{m_a^2} \ll 1$ . These results are well known [16]. The || polarized photon mixes with the axion. This means that the polarization plane will rotate, unless the photon polarization is initially exactly parallel or perpendicular to the magnetic field. The difference in frequency between the two ‘photon’ polarizations is, to a very good degree of approximation, equal to

$$\Delta\omega_\gamma = \omega_2 - \omega_1 \simeq \frac{b^2k}{2m_a^2} \quad (16)$$

and as is well known leads to the phenomenon of birefringence. We have identified as corresponding to ‘photons’ the two modes that if  $b = 0$  reduce to the two usual polarization modes. These are the two modes that will be relevant to us if  $\eta_0 \neq 0$ . The third frequency,  $\omega_a$ , is dominated by  $m_a$  with or without  $\eta_0$ . We will return to this issue shortly.

Let us now do some numerics. We shall be basically interested in the possibility of detecting this frequency difference using laser interferometry, for which typically  $k$  and  $\omega$  are  $\sim 1$  eV. For the largest values of  $b$  and  $1/m_a$  previously discussed the previous expression gives

$$\frac{\Delta\omega_\gamma}{\omega_\gamma} \simeq 10^{-16} \quad (17)$$

Small as this quantity may seem, laser interferometry is extremely precise and Michelson-Morley type experiments are capable of achieving a relative error as small as  $10^{-17}$  using heterodyne interferometry techniques[23]. The PVLAS collaboration claims that a sensitivity of order  $10^{-20}$  in the difference of refraction indices is ultimately achievable [24]. See also [25]

It must be said that it is not consistent with Peccei-Quinn axions to assume large values for  $b$  and for  $1/m_a$  simultaneously as  $b \sim 1/f_a$  and  $f_a$  and  $m_a$  are related by the PCAC relation  $f_a m_a \simeq \text{constant}$ ; therefore the current experimental sensitivity may not be enough because frequency differences of the order of  $10^{-22}$  eV or less are more likely for Peccei-Quinn axions, but it is surely relevant for other kinds of axion-like particles. The sensitivity could be enhanced by being able to reproduce the experiment with even larger magnetic fields<sup>4</sup>, a possibility that cannot be ruled out as such high intensity would be required only in a small volume (by performing  $N \gg 1$  reflections).

Let us now explore the situation where both the CAB and the magnetic field are present. We choose to work with the linear polarization basis. Again, in each time interval we can define  $(a, if_\parallel, f_\perp) = e^{i\omega t}(x, iX_\parallel, X_\perp)$ . Then the equations in matrix form are

$$\begin{pmatrix} -\omega^2 + k^2 + m_a^2 & \omega b & 0 \\ \omega b & -\omega^2 + k^2 & -\eta_0 k \\ 0 & -\eta_0 k & -\omega^2 + k^2 \end{pmatrix} \begin{pmatrix} x \\ iX_\parallel \\ X_\perp \end{pmatrix} = \begin{pmatrix} 0 \\ 0 \\ 0 \end{pmatrix}, \quad (18)$$

---

<sup>4</sup> Non-destructive magnetic fields close to 100 T have been achieved. This would enhance the sensitivity by a factor 100.

and involve a full three-way mixing as previously mentioned. The proper frequencies of the system turn out to be

$$\begin{aligned}\omega_a^2 &= k^2 + \frac{m_a^2 + b^2}{3} + 2\sqrt{Q} \cos \phi, \\ \omega_1^2 &= k^2 + \frac{m_a^2 + b^2}{3} - \sqrt{Q} (\cos \phi + \sqrt{3} \sin \phi), \\ \omega_2^2 &= k^2 + \frac{m_a^2 + b^2}{3} - \sqrt{Q} (\cos \phi - \sqrt{3} \sin \phi),\end{aligned}\tag{19}$$

where

$$\begin{aligned}Q &= \left( \frac{m_a^2 + b^2}{3} \right)^2 + \frac{1}{3} k^2 (b^2 + \eta_0^2), \\ \phi &= \frac{1}{3} \arctan \frac{\sqrt{Q^3 - R^2}}{R}, \\ R &= \frac{1}{54} (m_a^2 + b^2) [2m^4 + b^2(9k^2 + 4m_a^2 + 2b^2)] - \frac{1}{6} \eta_0^2 k^2 (2m_a^2 - b^2).\end{aligned}\tag{20}$$

It can be observed that they depend only on even powers of  $\eta_0$ , so they are not altered when  $\eta(t)$  changes sign. According to the discussion at the end of section II the limit  $\eta_0 \ll b \ll \{m_a, k\}$  is quite reasonable. The approximate expressions in this limit are

$$\begin{aligned}\omega_a^2 &\approx (k^2 + m_a^2) \left( 1 + \frac{b^2}{m_a^2} \right), \\ \omega_1^2 &\approx k^2 - k \sqrt{\eta_0^2 + \left( \frac{b^2 k}{2m_a^2} \right)^2} - \frac{b^2 k^2}{2m_a^2}, \\ \omega_2^2 &\approx k^2 + k \sqrt{\eta_0^2 + \left( \frac{b^2 k}{2m_a^2} \right)^2} - \frac{b^2 k^2}{2m_a^2}.\end{aligned}\tag{21}$$

The presence of the CAB introduces an additional splitting in the photon frequencies when compared to the case previously discussed, where the CAB is absent (Eq. (16))

$$\Delta\omega_\gamma = \omega_2 - \omega_1 \approx \sqrt{\eta_0^2 + \left( \frac{b^2 k}{2m_a^2} \right)^2}\tag{22}$$

or

$$\frac{\Delta\omega_\gamma}{\omega_\gamma} \approx \sqrt{\frac{\eta_0^2}{k^2} + \left( \frac{b^2}{2m_a^2} \right)^2}\tag{23}$$

Note that both effects add up and that the importance of the CAB is reinforced at very low frequencies, high axion masses or weak magnetic fields. When the effect of  $\eta(t)$  dominates, the difference in frequencies does not strongly depend directly on the axion mass.

For each value of the frequency, the eigenvectors that solve the system are

$$\omega_a : \begin{pmatrix} 1 \\ \frac{b\sqrt{k^2 + m_a^2}}{m_a^2} \\ -\frac{\eta_0 b k \sqrt{k^2 + m_a^2}}{m_a^4} \end{pmatrix}, \quad \omega_1 : \begin{pmatrix} -\frac{bk}{m_a^2} \\ 1 \\ \varepsilon \end{pmatrix}, \quad \omega_2 : \begin{pmatrix} \frac{bk}{m_a^2} \varepsilon \\ -\varepsilon \\ 1 \end{pmatrix}, \quad (24)$$

where

$$\varepsilon = \frac{\eta_0}{\sqrt{\eta_0^2 + \left(\frac{b^2 k}{2m_a^2}\right)^2 + \frac{b^2 k}{2m_a^2}}}. \quad (25)$$

Note that the above eigenvectors are written in the basis described in (9) that includes an imaginary unit for the parallel component. Therefore the eigenvectors for  $\omega_{1,2}$  correspond to photon states elliptically polarized with ellipticity <sup>5</sup>  $|\varepsilon|$ . In addition, unless exactly aligned to the magnetic field there will be a change in the angle of polarization. We will return to this in section VI.

We also note that the above value for  $\varepsilon$  correspond to the ellipticity of the eigenmodes. In section VI we will discuss the evolution of the ellipticity of photon state that is initially polarized, which is a different problem and probably is more relevant from an experimental point of view.

## V. NUMERICAL RESULTS

Let us now try to get some intuition on the relevance of the different magnitudes entering in the expressions for the differential frequency  $\Delta\omega_\gamma$  and the ellipticity.

There are two different limits we can study, depending of which term in the square root in (22) dominates. If  $\frac{\eta_0}{k} \ll \frac{b^2}{2m_a^2}$  we have  $\varepsilon \approx \frac{\eta_0 m_a^2}{b^2 k}$ . The ellipticity of the eigenmodes is small, so the proper modes are almost linearly polarized photons.

In the case  $\frac{\eta_0}{k} \gg \frac{b^2}{2m_a^2}$  we have  $\varepsilon \approx \text{sign}(\eta_0) \left(1 - \frac{b^2 k}{2|\eta_0| m_a^2}\right)$ . Now the ellipticity of the eigenmodes is close to 1 so the proper modes are almost circularly polarized. We see that while the proper frequencies depend only on the square of  $\eta_0$  (and therefore do not change as we go from one time interval to the next) the eigenvectors do change.

---

<sup>5</sup> Ellipticity is the ratio of the minor to major axes of the ellipse.

As previously discussed it is conceivable that the frequency difference (22) may be measurable in an interferometry experiment. Its values in the two discussed limits are

$$\Delta\omega_\gamma \approx \frac{b^2 k}{2m_a^2} + \frac{2\eta_0^2 m_a^2}{b^2 k} \quad \text{for} \quad \frac{\eta_0}{k} \ll \frac{b^2}{2m_a^2}, \quad (26)$$

and

$$\Delta\omega_\gamma \approx \eta_0 + \frac{1}{2\eta_0} \left( \frac{b^2 k}{2m_a^2} \right)^2 \quad \text{for} \quad \frac{\eta_0}{k} \gg \frac{b^2}{2m_a^2}. \quad (27)$$

As can be seen, the frequency splitting increases with the momentum and the magnetic field, which reflects the presence of axions, but not of the CAB. If the effects of the CAB are to be detected one should be in the second situation.

Extreme care has to be exercised when using approximate formulae based on series expansions in  $b$  or  $\eta_0$  because there is a competition among dimensionful quantities, several of which take rather small values.

In figures 3 and 4 we give some numerical results for two rather extreme values of  $m_a$  and  $\eta_0$ , within our hypothesis. The first figure depicts the logarithm (in decimal base) of the difference of frequencies  $\Delta\omega_\gamma$  plotted as a function of  $k$  and the reduced magnetic field  $b$ . The second figure shows the dependence of the ellipticity of the eigenmodes on the same parameters also given in a decimal logarithmic scale. The figures show different regions of the allowed parameter space where the effects due to the CAB dominate.

## VI. ELLIPTICITY AND ROTATION IN AN AXION BACKGROUND

Given that the magnetic field mixes the photon with the axion it is natural to ask whether one should identify the “photon” with two of the proper modes in the magnetic field as we did when writing (16). However, only the true photon component of the proper modes excites electrons and gets reflected in mirrors. In order not to get mixed-up among the two possible bases, it is very useful to consider the electric field correlator, easily derived from the resummed photon propagator derived in [14]. Using that  $\vec{k} \cdot \vec{B} = 0$ , we get in momentum space

$$D_{ij}^E(\omega, k) = -\frac{ig_{ij}\omega^2}{\omega^2 - k^2} - \frac{i\omega^4 b_i b_j}{(\omega^2 - k^2)[(\omega^2 - k^2)(\omega^2 - k^2 - m_a^2) - \omega^2 b^2]}. \quad (28)$$

Notice the rather involved structure of the dispersion relation implied in the second term, which is only present when  $b \neq 0$ , while the first piece corresponds to the unperturbed propagator. The zeros of the denominator are actually the proper frequencies  $\omega_a, \omega_1$  and

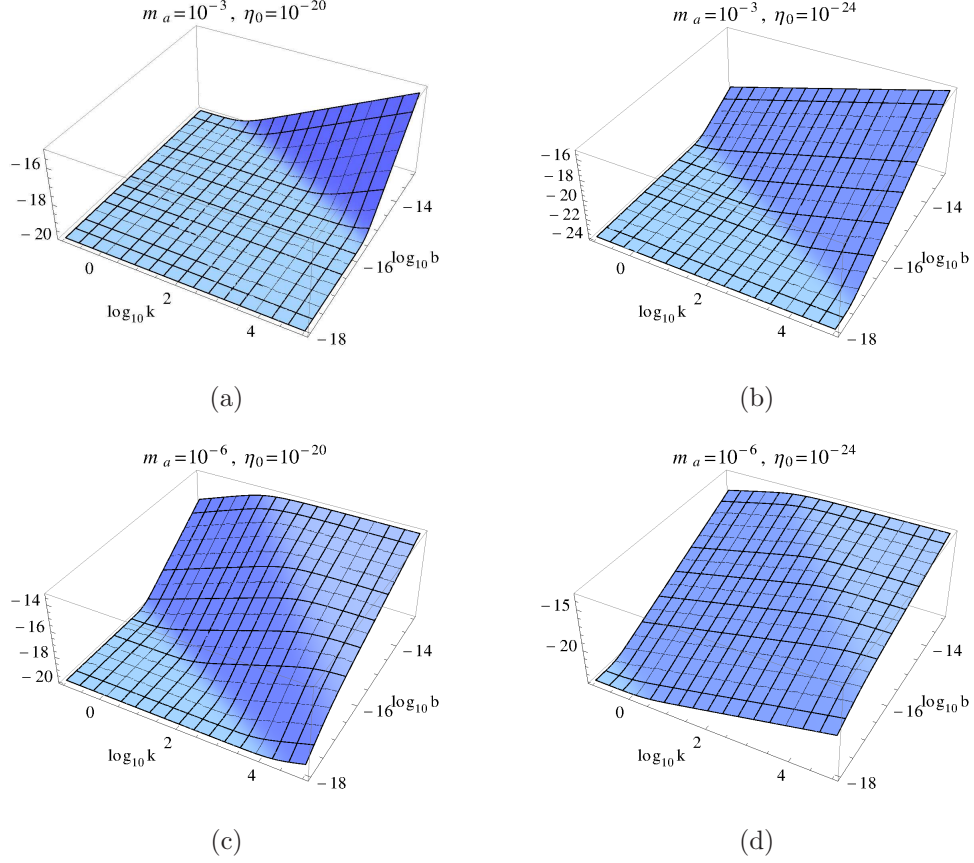


FIG. 3:  $\log_{10} \Delta\omega_\gamma$  as a function of the  $b = gB$  and the wave vector  $k$  for different values of  $m_a$  and  $|\eta_0|$ . (a):  $m_a = 10^{-3}$  eV,  $|\eta_0| = 10^{-20}$  eV, (b):  $m_a = 10^{-3}$  eV,  $|\eta_0| = 10^{-24}$  eV, (c):  $m_a = 10^{-6}$  eV,  $|\eta_0| = 10^{-20}$  eV, and (d):  $m_a = 10^{-6}$  eV,  $|\eta_0| = 10^{-24}$  eV.

$\omega_2$ . We consider the propagation of plane waves moving in the  $\hat{x}$  direction. The Fourier transform with respect to the spatial component will describe the space evolution of the electric field. We decompose

$$\frac{1}{(\omega^2 - k^2)[(\omega^2 - k^2)(\omega^2 - k^2 - m^2) - \omega^2 b^2]} = \frac{A}{k^2 - \omega^2} + \frac{B}{k^2 - F^2} + \frac{C}{k^2 - G^2}, \quad (29)$$

where  $\omega$ ,  $F$  and  $G$  are the roots of the denominator

$$\begin{aligned} F^2 &= \omega^2 - \frac{m_a^2}{2} + \frac{1}{2}\sqrt{m_a^4 + 4\omega^2 b^2} \approx \left(1 + \frac{b^2}{m_a^2}\right)\omega^2, \\ G^2 &= \omega^2 - \frac{m_a^2}{2} - \frac{1}{2}\sqrt{m_a^4 + 4\omega^2 b^2} \approx \left(1 - \frac{b^2}{m_a^2}\right)\omega^2 - m_a^2, \end{aligned} \quad (30)$$

and

$$A = -\frac{1}{\omega^2 - F^2} \frac{1}{\omega^2 - G^2} = \frac{1}{\omega^2 b^2},$$

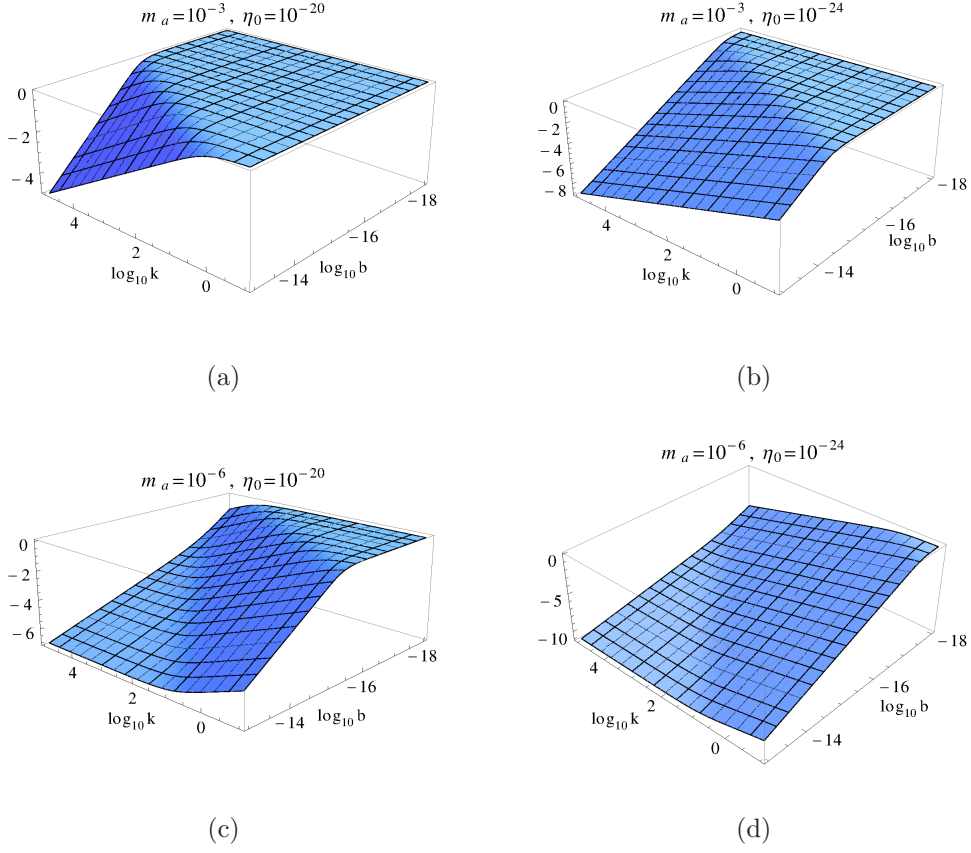


FIG. 4: Ellipticity:  $\log_{10} \varepsilon$  as a function of the  $b = gB$  and the wave vector  $k$  for the values  $m_a = 10^{-3}, 10^{-6}$  eV and  $|\eta_0| = 10^{-20}, 10^{-24}$  eV. Labels as in Figure 3

$$\begin{aligned}
 B &= -\frac{1}{F^2 - \omega^2} \frac{1}{F^2 - G^2} \approx -\frac{1}{\omega^2 b^2} \left( 1 - \frac{\omega^2 b^2}{m^4} \right), \\
 C &= -\frac{1}{G^2 - \omega^2} \frac{1}{G^2 - F^2} \approx -\frac{1}{m_a^4}.
 \end{aligned} \tag{31}$$

The space Fourier transform of the electric field propagator is

$$\begin{aligned}
 D_{ij}^E(\omega, x) &= -g_{ij} \frac{\omega}{2} e^{i\omega x} + \frac{\omega^4}{2} b_i b_j \left( \frac{A}{\omega} e^{i\omega x} + \frac{B}{F} e^{iFx} + \frac{C}{G} e^{iGx} \right) \\
 &= \frac{\omega}{2} e^{i\omega x} \left[ -g_{ij} + \omega^3 b_i b_j \left( \frac{A}{\omega} + \frac{B}{F} e^{i(F-\omega)x} + \frac{C}{G} e^{i(G-\omega)x} \right) \right],
 \end{aligned} \tag{32}$$

where  $x$  is the travelled distance. After factoring out the exponential  $e^{i\omega x}$  we consider the relative magnitude of the differential frequencies  $\Delta\omega_\gamma = F - \omega$  and  $G - \omega$ . The latter is much larger and for  $m_a^2 x / 2\omega \gg 1$  the corresponding exponential could be dropped. This approximation was made in [14] and for the range of axion masses envisaged here and  $\omega \sim 1$  eV is valid for all astrophysical and most terrestrial experiments. As for the exponential

containing  $F - \omega$ , we can safely expand it for table-top experiments and retain only the first non-trivial term. In this case, the leading terms in the propagator are

$$D_{ij}^E(\omega, x) \approx \frac{\omega}{2} e^{i\omega x} \left[ -g_{ij} + \hat{b}_i \hat{b}_j \left( \frac{\omega^2 b^2}{m_a^4} - i \frac{\omega b^2 x}{2m_a^2} \right) \right], \quad (33)$$

where  $\hat{b}$  is a unitary vector in the direction of the magnetic field. For very light axion masses, neglecting the  $e^{i(G-\omega)x}$  exponential cannot be justified for table top experiments. Then one should use a slightly more complicated propagator, namely

$$D_{ij}^E(\omega, x) \approx \frac{\omega}{2} e^{i\omega x} \left\{ -g_{ij} + \hat{b}_i \hat{b}_j \frac{\omega^2 b^2}{m_a^4} \left[ 1 - \cos \frac{m_a^2 x}{2\omega} + i \left( \sin \frac{m_a^2 x}{2\omega} - \frac{m_a^2 x}{2\omega} \right) \right] \right\}. \quad (34)$$

These expressions agree in the appropriate limits with the ones in [16].

When a CAB is considered the electric field propagator changes to

$$D_{ij}^E(\omega, k) = -i\omega^2 \left( \frac{P_{+ij}}{\omega^2 - k^2 - \eta_0 k} + \frac{P_{-ij}}{\omega^2 - k^2 + \eta_0 k} \right) - i\omega^4 \frac{b_i b_j}{(\omega^2 - k^2)[(\omega^2 - k^2)(\omega^2 - k^2 - m_a^2) - \omega^2 b^2]}. \quad (35)$$

This expression differs from the one presented in formula (75) of [14] in that (a) only the leading contribution to the term proportional to the magnetic field is retained and (b) the piece independent of the magnetic field contains (unlike in [14]) the modifications from the CAB. See the appendix for a complete discussion. The external magnetic field can be set to zero in the previous expressions, if desired.

By projecting on suitable directions and taking the modulus square of the resulting quantity, the following expression for the angle of maximal likelihood (namely, the one where it is more probable to find the direction of the rotated electric field) as a function of the distance  $x$  can be found

$$\alpha(x) = \beta - \frac{\eta_0 x}{2} - \frac{\epsilon}{2} \sin 2\beta, \quad (36)$$

where  $\beta$  is the initial angle that the oscillation plane of the electric field forms with the background magnetic field and

$$\epsilon \approx -\frac{\omega^2 b^2}{m_a^4} \left( 1 - \cos \frac{m_a^2 x}{2\omega} \right). \quad (37)$$

From the results in the appendix, the ellipticity turns out to be

$$e = \frac{1}{2} |\varphi \sin 2\beta|, \quad \varphi \approx \frac{\omega^2 b^2}{m_a^4} \left( \frac{m_a^2 x}{2\omega} - \sin \frac{m_a^2 x}{2\omega} \right). \quad (38)$$

For small distances,  $\frac{m_a^2 x}{2\omega} \ll 1$  we can expand the trigonometric functions to get

$$\epsilon \approx -\frac{b^2 x^2}{8}, \quad \varphi \approx \frac{m^2 b^2 x^3}{48\omega}. \quad (39)$$

If this limit is not valid, we have instead

$$\epsilon \approx -\frac{\omega^2 b^2}{m^4}, \quad \varphi \approx \frac{\omega b^2 x}{2m^2}. \quad (40)$$

It can be noted that the effect of the magnetic field always comes with the factor  $\sin 2\beta$ , which means that it disappears if the electric field is initially parallel ( $\beta = 0$ ) or perpendicular ( $\beta = \pi/2$ ) to the external magnetic field.

The results of [16], which we reproduce in the case where  $\eta_0 = 0$  are known to be in agreement with later studies such as [19], which has somehow become a standard reference in the field. However, their approach is not adequate to deal with time dependent backgrounds and therefore it is not easy to reinterpret the results derived in the present work when a non-vanishing CAB is present in the language of [19].

If  $\eta_0 \neq 0$  a rotation is present even in the absence of a magnetic field. This is a characteristic footprint of the CAB. This ‘anomalous’ rotation attempts to bring the initial polarization plane, arbitrary in principle, with one of the two elliptic eigenmodes. In the case where the effect of  $\eta_0$  dominates, the eigenmodes are almost circularly, rather than linearly, polarized so the changes in the plane of polarization are of order one. The effect is independent of the frequency. Equation (36) shows however that the process of rotation due to the CAB is very slow, with a characteristic time  $\eta_0^{-1}$ .

Typically in interferometric-type experiments the laser light is made to bounce and folded many times. Formula (36) can be used each time that the light travels back and forth. When this happens,  $\beta$  changes sign and so does  $\sin 2\beta$ . Since  $\epsilon$  is always negative, the effect of the magnetic field is always to increase  $\beta$  in absolute value (i.e. moving the polarization plane away from the magnetic field). So in this sense, the rotation accumulates, contrary to what is said in [16]. The situation is different for the CAB term. It does not change sign when  $\beta$  does, so its effect compensates each time the light bounces. However, recall that  $\eta_0$  changes sign with a half-period  $\pi m_a^{-1}$  so the effect could be accumulated by tuning the length between each bounce. The range of values of  $\pi m_a^{-1}$  makes this perhaps a realistic possibility for table-top experiments (we are talking here about lengths of centimeters or meters for most accepted values of  $m_a$ ).

Observing a net rotation of the initial plane of polarization when the magnetic field is absent (or very small) would be a clear signal of the collective effect of a CAB. On the contrary, a non-zero value for  $\eta_0$  does not contribute at leading order to a change in the ellipticity (and subleading corrections are very small). In [27] the authors discuss in some detail the different backgrounds, all of which are very small with the exception of the dichroism originating from the experimental apparatus itself [28]. Ways of partially coping with these experimental limitations are discussed in the previous reference.

## VII. CONCLUSIONS

In this work we have extended the analysis of axion-photon mixing in the presence of an external magnetic field to the case where a cold axion background (CAB) is present too. The mixing is then substantially more involved and the two photon polarizations mix even without a magnetic field. In particular in our results we can take the limit where the magnetic field vanishes.

We have made one approximation that we believe is not essential, namely we have approximated the assumed sinusoidal variation in time of the CAB by a piece-wise linear function; resulting in a fully analytically solvable problem. We believe that this captures the basic physics of the problem and we expect only corrections of  $\mathcal{O}(1)$  in some numerical coefficients but no dramatic changes in the order-of-magnitude estimates.

The existence of some momentum gaps due to the periodic time dependence of the CAB and its implications has been reviewed too. It seems challenging to design experiments to verify or falsify their existence, but in any case they are unavoidable if dark matter is explained in terms of an axion background; in fact it would possibly be the most direct evidence of the existence of a CAB.

We have obtained the proper modes and their ellipticities and we have analyzed in detail the evolution of the system. Regarding the proper modes and ellipticities, the presence of a non-vanishing CAB adds to the difference in their propagation (birefringence) and should enhance the effect, even though the amount of the enhancement is needless to say very modest. It should be said that CAB-related effects dominate in some regions of the allowed parameter space. We have also studied the possible presence of accumulative effects that might enhance the rotation of the instantaneous plane of polarization. This would also be a

genuine CAB effect.

In order to analyze the evolution of the system we have made use of the two point function for the electric field, that correlates the value at  $x = 0$  with the one at a given value for  $x$ . We find this a convenient and compact way of treating this problem.

### Acknowledgements

This work is supported by grants FPA2010-20807, 2009SGR502 and Consolider grant CSD2007-00042 (CPAN). A. Renau acknowledges the financial support of a FPU pre-doctoral grant. It is a pleasure to thank several of the participants in the 9th Patras Workshop for discussions.

- 
- [1] R.D. Peccei, H.R. Quinn, Phys. Rev. Lett. 38 (1977) 1440; S. Weinberg, Phys. Rev. Lett. 40 (1978) 223; F. Wilczek, Phys. Rev. Lett. 40 (1978) 279.
  - [2] L. Abbott and P. Sikivie, Phys. Lett. B 120, 133 (1983); M. Dine and W. Fischler, Phys. Lett. B 120, 137 (1983).
  - [3] M. Kuster, G. Raffelt and B. Beltran (eds), Lecture Notes in Physics 741 (2008).
  - [4] P. Sikivie and Q. Yang, Phys. Rev. Lett. 112, 068103 (2009).
  - [5] M. Dine, W. Fischler and M. Srednicki, Phys. Lett. B, 104, 199 (1981); A.R. Zhitnitsky, Sov. J. Nucl. Phys. 31, 260 (1980); J. E. Kim, Phys. Rev. Lett. 43, 103 (1979); M. A. Shifman, A. I. Vainshtein and V. I. Zakharov, Nucl. Phys. B 166, 493 (1980).
  - [6] J. Beringer et al. (Particle Data Group), PR D86, 010001 (2012)
  - [7] A.H. Corsico et al, JCAP 1212 (2012) 010.
  - [8] E. Arik et al. (CAST collaboration), J. Cosmo. Astropart. Phys. 02, 008 (2009)
  - [9] S. J. Asztalos et al. (ADMX collaboration), Nuclear Instruments and Methods in Physics Research A 656, 39-44 (2011)
  - [10] I. G. Irastorza et al. (IAXO collaboration), JCAP 1106 (2011) 013
  - [11] R. Bähre et al. (ALPS collaboration), JINST 1309, T09001 (2013)
  - [12] A. A. Andrianov, D. Espriu, F. Mescia and A. Renau, Phys. Lett. B 684 (2010) 101.
  - [13] D. Espriu, F. Mescia, A. Renau, JCAP 1108 (2011) 002.

- [14] D. Espriu and A. Renau, Phys. Rev. D85 (2012) 025010.
- [15] S. Adler, Ann. Phys (NY) 67 (1971) 599; G. Raffelt and L. Stodolsky, Phys. Rev. D 37, 1237 (1988).
- [16] L. Maiani, R. Petronzio and E. Zavattini, Phys. Lett. B 175, 359 (1987)
- [17] D. Espriu and A. Renau, in Proceedings of the 9th Patras Workshop, Mainz, June 2013 [arXiv:1309.6948].
- [18] H. Euler and B. Kochel, Naturwiss. 23 (1935) 246; W. Heisenberg and H. Euler, Z. Phys. 98 (1936) 718.
- [19] G. Raffelt and L. Stodolsky, Phys. Rev. D37, 1237 (1988).
- [20] See e.g. Particle Dark Matter: Observations, Models and Searches, G. Bertone (ed.), Cambridge University Press (2010).
- [21] G. Zavattini et al. (PVLAS collaboration), Phys. Rev. D77 (2008) 032006.
- [22] A. A. Andrianov, D. Espriu, P. Giacconi and R. Soldati, JHEP 0909:057,2009.
- [23] C. Eisele, A. Y. Nevsky and S. Schiller, Physical Review Letters 103 (2009) 090401; S. Herrmann et al., Physical Review D 80 (2009) 105011.
- [24] G. Zavattini et al. (PVLAS collaboration) Int. J. Mod. Phys. A27 (2012) 1260017.
- [25] H. Tam and Q. Yang, Phys. Lett. B 716 (2012) 435.
- [26] M. Born and W. Wolf, Principles of optics, 4th edition, Pergamon Press, Oxford (1970).
- [27] M. Ahlers, J. Jaeckel and A. Ringwald, Phys. Rev. D79, 075017 (2009).
- [28] G. Zavattini et al., Applied Physics B - Lasers and Optics 83, 571 (2006).

## Appendix A: Propagator

Considering only the spatial components, eq. (52) of [14] becomes:

$$\mathcal{D}^{ij}(\omega, k) = D^{ij} + i\omega^2 \left\{ \frac{b^i b^j}{(k^4 - \eta_0^2 \vec{k}^2)(k^2 - m_a^2) - \omega^2 k^2 b^2} + \frac{i\eta_0 k^2 (b^i q^j - q^i b^j)}{(k^4 - \eta_0^2 \vec{k}^2)[(k^4 - \eta_0^2 \vec{k}^2)(k^2 - m_a^2) - \omega^2 k^2 b^2]} \right\}, \quad (\text{A1})$$

where

$$D^{ij} = -i \left( \frac{P_+^{ij}}{k^2 - \eta_0 |\vec{k}|} + \frac{P_-^{ij}}{k^2 + \eta_0 |\vec{k}|} \right), \quad \vec{q} = (\vec{b} \times \vec{k}) \quad (\text{A2})$$

and the projectors  $P_{\pm}$  have been defined in [22]. Terms proportional to  $k^i k^j$  have been dropped, since we are interested in contracting the propagator with a photon polarization vector. The roots of the denominators are  $|\vec{k}| = F_j$ , with

$$\begin{aligned} F_{1,2}^2 &= \omega^2 + \frac{\eta_0^2}{2} \mp \frac{\eta_0}{2} \sqrt{4\omega^2 + \eta_0^2} \approx \omega^2 \mp \omega\eta_0, \\ F_{3,4}^2 &= \omega^2 - \frac{m_a^2 - \eta_0^2}{3} + \sqrt{W}(\cos \chi \mp \sqrt{3} \sin \chi), \\ F_5^2 &= \omega^2 - \frac{m_a^2 - \eta_0^2}{3} - 2\sqrt{W} \cos \chi. \end{aligned} \quad (\text{A3})$$

$$\begin{aligned} W &\approx \left(\frac{m_a^2}{3}\right)^2 \left(1 + \frac{3\omega^2 b^2}{m_a^4}\right), \\ \chi &\approx \frac{1}{m_a^2} \sqrt{3} \omega \xi, \\ \xi &\approx \left(1 + \frac{9\omega^2 b^2}{2m_a^4}\right)^{-1} \sqrt{\eta_0^2 + \left(\frac{\omega b^2}{2m_a^2}\right)^2 + \left(\frac{\omega^2 b^3}{m_a^4}\right)^2}. \end{aligned} \quad (\text{A4})$$

$F_1$  and  $F_2$  correspond to the pieces with  $P_+$  and  $P_-$ , respectively. The piece proportional to  $b^i b^j$  has poles at  $F_{3,4,5}^2$  and the last piece contains all five poles. We decompose the denominators in simple fractions:

$$\frac{1}{(k^4 - \eta_0^2 \vec{k}^2)(k^2 - m_a^2) - \omega^2 k^2 b^2} = \sum_{l=3}^5 \frac{A_l}{\vec{k}^2 - F_l^2}, \quad (\text{A5})$$

with

$$A_l = \frac{-1}{\prod_{m \neq l, 1, 2} (F_l^2 - F_m^2)}, \quad l = 3, 4, 5 \quad (\text{A6})$$

and

$$\frac{k^2}{(k^4 - \eta_0^2 \vec{k}^2)[(k^4 - \eta_0^2 \vec{k}^2)(k^2 - m_a^2) - \omega^2 k^2 b^2]} = \sum_{l=1}^5 \frac{\tilde{A}_l}{\vec{k}^2 - F_l^2}, \quad (\text{A7})$$

with

$$\tilde{A}_l = \frac{-(\omega^2 - F_l^2)}{\prod_{m \neq l} (F_l^2 - F_m^2)}, \quad l = 1, \dots, 5. \quad (\text{A8})$$

Then,

$$\begin{aligned} \mathcal{D}^{ij}(\omega, \vec{k}) &= i \left( \frac{P_+^{ij}}{\vec{k}^2 - F_1^2} + \frac{P_-^{ij}}{\vec{k}^2 - F_2^2} \right) \\ &\quad + i\omega^2 b^2 \left[ \hat{b}^i \hat{b}^j \sum_{l=3}^5 \frac{A_l}{\vec{k}^2 - F_l^2} + i\eta_0 (\hat{b}^i \hat{q}^j - \hat{q}^i \hat{b}^j) \sum_{l=1}^5 \frac{|\vec{k}| \tilde{A}_l}{\vec{k}^2 - F_l^2} \right] \end{aligned} \quad (\text{A9})$$

We choose the axes so that

$$\hat{k} = (1, 0, 0), \quad \hat{b} = (0, 1, 0), \quad \hat{q} = (0, 0, -1). \quad (\text{A10})$$

The propagator in position space is, after dropping an overall factor,

$$d^{ij}(\omega, x) \approx (P_+^{ij} + P_-^{ij}) \cos\left(\frac{\eta_0 x}{2}\right) + i(P_+^{ij} - P_-^{ij}) \sin\left(\frac{\eta_0 x}{2}\right) \\ + \hat{b}^i \hat{b}^j \sum_{l=3}^5 a_l e^{i\alpha_l x} - i(\hat{b}^i \hat{q}^j - \hat{q}^i \hat{b}^j) \sum_{l=1}^5 \tilde{a}_l e^{i\alpha_l x}, \quad (\text{A11})$$

where

$$a_l = \frac{\omega^3 b^2 A_l}{F_l}, \quad \tilde{a}_l = \omega^3 b^2 \eta_0 \tilde{A}_l, \quad \alpha_l = F_l - \omega. \quad (\text{A12})$$

All the  $\alpha_l$  are proportional to  $\eta_0$  or  $b^2$ , except for  $\alpha_5 \approx -\frac{m_a^2}{2\omega}$ . Restricting ourselves only to  $y - z$  components, we can write  $d(\omega, x)$  in matrix form.

$$P_{+j}^i + P_{-j}^i = \begin{pmatrix} 1 & 0 \\ 0 & 1 \end{pmatrix}, \quad (\text{A13})$$

$$i(P_{+j}^i - P_{-j}^i) = \begin{pmatrix} 0 & 1 \\ -1 & 0 \end{pmatrix}, \quad (\text{A14})$$

$$\hat{b}^i \hat{b}_j = \begin{pmatrix} -1 & 0 \\ 0 & 0 \end{pmatrix}, \quad (\text{A15})$$

$$-i(\hat{b}^i \hat{q}_j - \hat{q}^i \hat{b}_j) = \begin{pmatrix} 0 & -i \\ i & 0 \end{pmatrix}. \quad (\text{A16})$$

If we write

$$\sum_l a_l e^{i\alpha_l x} = -(\epsilon + i\varphi), \quad i \sum_l \tilde{a}_l e^{i\alpha_l x} = -(\tilde{\epsilon} + i\tilde{\varphi}), \quad (\text{A17})$$

we have

$$d_j^i(\omega, x) = \begin{pmatrix} \cos \frac{\eta_0 x}{2} + \epsilon + i\varphi & \sin \frac{\eta_0 x}{2} + \tilde{\epsilon} + i\tilde{\varphi} \\ -(\sin \frac{\eta_0 x}{2} + \tilde{\epsilon} + i\tilde{\varphi}) & \cos \frac{\eta_0 x}{2} \end{pmatrix} \quad (\text{A18})$$

## Appendix B: Ellipticity and rotation

The quantities appearing in (A18) are

$$\epsilon \approx -\frac{\omega^2 b^2}{m_a^4} \left(1 - \cos \frac{m_a^2 x}{2\omega}\right), \quad \varphi \approx \frac{\omega^2 b^2}{m_a^4} \left(\frac{m_a^2 x}{2\omega} - \sin \frac{m_a^2 x}{2\omega}\right), \quad (\text{B1})$$

while  $\tilde{\epsilon}$  and  $\tilde{\varphi}$  are both proportional to  $b^2 \eta_0$ , so they are negligible.

In the limit  $\frac{m_a^2 x}{2\omega} \ll 1$  we have

$$\epsilon \approx -\frac{b^2 x^2}{8}, \quad \varphi \approx \frac{m_a^2 b^2 x^3}{48\omega} \quad (\text{B2})$$

whereas if  $\frac{m_a^2 x}{2\omega} \gg 1$  the trigonometric functions oscillate rapidly and can be dropped:

$$\epsilon \approx -\frac{\omega^2 b^2}{m_a^4}, \quad \varphi \approx \frac{\omega b^2 x}{2m_a^2}. \quad (\text{B3})$$

Eq. (B2) agrees with eq. 16 of [16] (although their  $k^2$  in the denominator should be only  $k$ , the dimensions do not fit otherwise). Eq. (B3) agrees with their eq. (20,21), at least to second order in  $b$ .

If we start with a polarization  $\vec{n}_0 = (\cos \beta, \sin \beta)$ , after a distance  $x$  we have

$$n_x^i = d_j^i(x) n_0^j = \begin{pmatrix} \cos(\beta - \frac{\eta_0 x}{2}) + (\epsilon + i\varphi) \cos \beta \\ \sin(\beta - \frac{\eta_0 x}{2}) \end{pmatrix} \quad (\text{B4})$$

Following section 1.4 of [26], this vector describes a polarization at an angle

$$\alpha \approx \beta - \frac{\eta_0 x}{2} - \frac{\epsilon}{2} \sin 2\beta \quad (\text{B5})$$

and with ellipticity

$$e = \frac{1}{2} |\varphi \sin 2\beta|. \quad (\text{B6})$$

This ellipticity differs from the one described in [16] by the factor of  $\sin 2\beta$ .

Quantum mechanically the quantity that is relevant is not the amplitude itself, but the modulus squared of it. From this, the probability of finding an angle  $\alpha$  given an initial angle  $\beta$  will be

$$P(\alpha, \beta) = |\epsilon'_i d^{ij} \epsilon_j|^2 \approx \cos^2 \left( \alpha - \beta + \frac{\eta_0 x}{2} \right) + 2\epsilon \cos \left( \alpha - \beta + \frac{\eta_0 x}{2} \right) \cos \alpha \cos \beta. \quad (\text{B7})$$

The angle of maximum probability, satisfying  $\partial_\alpha P(\alpha, \beta) = 0$  is also, to first order,

$$\alpha = \beta - \frac{\eta_0 x}{2} - \frac{\epsilon}{2} \sin 2\beta. \quad (\text{B8})$$